Resistance to pentamidine is mediated by AdeAB, regulated by AdeRS, and influenced by growth conditions in *Acinetobacter baumannii* ATCC 17978

Felise G. Adams[1], Uwe H. Stroeher[1], Karl A. Hassan[2,#a], Shashikanth Marri[3], Melissa H. Brown[1*]

[1] College of Science and Engineering, Flinders University, Adelaide, SA, Australia

[2] Department of Chemistry and Biomolecular Sciences, Macquarie University, Sydney, NSW, Australia

[3] College of Medicine and Public Health, Flinders University, Adelaide, SA, Australia

[#a] Current address: Karl A. Hassan, School of Environmental and Life Science, University of Newcastle, Callaghan, NSW, Australia

[*]Corresponding author

Email: melissa.brown@flinders.edu.au (MHB)

Abstract

In recent years, effective treatment of infections caused by *Acinetobacter baumannii* has become challenging due to the ability of the bacterium to acquire or up-regulate antimicrobial resistance determinants. Two component signal transduction systems are known to regulate expression of virulence factors including multidrug efflux pumps. Here, we investigated the role of the AdeRS two component signal transduction system in regulating the AdeAB efflux system, determined whether AdeA and/or AdeB can individually confer antimicrobial resistance, and explored the interplay between pentamidine resistance and growth conditions in *A. baumannii* ATCC 17978. Results identified that deletion of *adeRS* affected resistance towards chlorhexidine and 4',6-diamidino-2-phenylindole dihydrochloride, two previously defined AdeABC substrates, and also identified an 8-fold decrease in resistance to pentamidine. Examination of Δ*adeA*, Δ*adeB* and Δ*adeAB* cells augmented results seen for Δ*adeRS* and identified a set of dicationic AdeAB substrates. RNA-sequencing of Δ*adeRS* revealed transcription of 290 genes were ≥2-fold altered compared to the wildtype. Pentamidine shock significantly increased *adeA* expression in the wildtype, but decreased it in Δ*adeRS*, implying that AdeRS activates *adeAB* transcription in ATCC 17978. Investigation under multiple growth conditions, including the use of Biolog phenotypic microarrays, revealed resistance to pentamidine in ATCC 17978 and mutants could be altered by bioavailability of iron or utilization of different carbon sources. In conclusion, the results of this study provide evidence that AdeAB in ATCC 17978 can confer intrinsic resistance to a subset of dicationic compounds and in particular, resistance to pentamidine can be significantly altered depending on the growth conditions.

Introduction

Acinetobacter baumannii causes a range of disease states including hospital-acquired pneumonia, blood stream, urinary, wound and bone infections, and is responsible for epidemic outbreaks of infection worldwide [1]. Such infections are often very difficult to treat due to the multidrug resistant (MDR) character of isolates displayed by this organism [2, 3]. In addition to the impressive propensity of the organism to acquire genetic elements carrying resistance determinants [2, 4, 5], up-regulation resulting in overproduction of resistance nodulation cell-division (RND) drug efflux systems through integration of insertion sequence elements or mutations in regulatory genes, has also been deemed a major contributor to the MDR phenotype [6-9]. The best studied RND efflux systems in *A. baumannii* include AdeABC [10], AdeFGH [11] and AdeIJK [12]. Of particular interest is the AdeABC system which affords resistance to diverse antibiotics, biocides and dyes [10, 13-15], and has gained attention due to its high incidence of over-expression across many MDR *A. baumannii* clinical isolates, primarily from incorporation of point mutations in the genes encoding its positive regulator, AdeRS [6, 8, 13, 16]. Typically RND pumps consist of three proteins that form a complex; the absence of any of these components renders the entire complex non-functional [17]. Interestingly, deletion of *adeC* in the *A. baumannii* strain BM4454 did not affect resistance towards two substrates of the pump suggesting that AdeAB can utilize an alternative outer membrane protein (OMP) to efflux antimicrobial compounds [13].

The genetic arrangement of the AdeABC system places *adeABC* in an operon that is divergently transcribed to the regulatory *adeRS* two component signal transduction system (TCSTS). Expression of *adeABC* occurs by binding of AdeR to a ten base-pair

direct repeat motif found within the intercistronic region separating these operons [18, 19]. Many clinical *A. baumannii* isolates harbor different genetic arrangements of the *adeRS* and *adeABC* operons [20], and whether regulation via AdeRS is conserved in these strains is not completely understood.

With an increase in infections caused by MDR isolates across many bacterial species, including *A. baumannii*, understanding mechanisms of resistance and how resistance to and evasion of treatments has evolved over time has become a key research topic. Furthermore, determining the impact of expression of resistance determinants within the host environment and its effect on the efficacy of therapeutic treatments has gained attention. For example, when *Pseudomonas aeruginosa* is grown using L-glutamate as the sole carbon source, resistance to the related compounds polymyxin B and colistin increased ≥ 25- and 9-fold, respectively [21]. Other studies have shown that the bioavailability of cations such as iron can have a drastic effect towards the resistance of a number of antimicrobials across a range of pathogenic bacterial species [22]. Despite *A. baumannii* being recognized as a major human pathogen, these types of studies are limited for this organism.

This study aimed to determine the regulatory role of the AdeRS TCSTS in *A. baumannii* ATCC 17978, a clinical isolate which only encodes the *adeAB* subunits and identify whether AdeA and or AdeB alone can confer antimicrobial resistance in the ATCC 17978 background. Phenotypic characterization of a constructed panel of deletion strains identified that alterations to the *adeRS* and *adeAB* operons of ATCC 17978 reduced resistance to a subset of dicationic compounds, including pentamidine. As a recent study highlighted the effectiveness of pentamidine in combination therapy to treat infections caused by Gram-negative pathogens [23], we sought to further examine

alternative mechanisms of pentamidine resistance in *A. baumannii*. The type of carbon source and availability of iron were identified as affecting pentamidine resistance, thereby revealing interconnectedness between metabolic and resistance strategies within this formidable pathogen.

Materials and methods

Bacterial strains, plasmids and growth conditions

A. baumannii ATCC 17978 [24] was obtained from the ATCC and is designated as wildtype (WT). Bacterial strains, plasmids and primers used in this study are summarized in S1 and S2 Tables, respectively. Bacterial strains were cultured using Luria-Bertani (LB) broth or LB agar plates, under aerobic conditions at 37°C, unless otherwise stated. Antibiotic concentrations used for selection were; ampicillin 100 mg/L, erythromycin (ERY) 25 mg/L, tetracycline 12 mg/L and gentamicin (GEN) 12.5 mg/L. All antimicrobial agents were purchased from Sigma with the exception of ampicillin which was purchased from AMRESCO.

M9 minimal medium agar plates were generated using a stock solution of 5 × M9 salts (200 mM $Na_2HPO_4.7H_2O$, 110 mM KH_2PO_4, 43 mM NaCl and 93 mM NH_4Cl) and subsequently diluted 1:5 and supplemented with 2 mM $MgSO_4$, 0.1 mM $CaCl_2$ and 0.4% (w/v) of various carbon sources on the day of use. M9 minimal medium was supplemented with 0.4% (w/v) of glucose, or succinic, fumaric, citric, α-ketoglutaric, pyruvic, glutamic or oxaloacetic acids. All carbon compounds were purchased from Sigma with the exception of citric and pyruvic acids which were purchased from Chem-

Supply (Gillman, Australia). For solid media, J3 grade agar (Gelita, Australia) was used at a final concentration of 1%.

Iron-chelated and iron-rich conditions were achieved by the addition of dipyridyl (DIP) or $FeSO_4.7H_2O$ (Scharlau) at final concentrations of 100 and 200 µM or 2.5 and 5 mM in Mueller-Hinton (MH) agar, respectively.

Antimicrobial susceptibility testing

The resistance profiles of WT and derivative strains were determined via broth microdilution methods [25] which were performed in duplicate with a minimum of three biological replicates using bacteria cultured in MH broth. Growth was monitored at 600 nm (OD_{600}) using a FLUOstar Omega spectrometer (BMG Labtech, Germany) after overnight incubation at 37°C.

For disk diffusion assays, strains were grown to mid-log phase in MH broth, diluted to OD_{600} = 0.1 in fresh MH broth and 100 µL plated onto MH agar plates on which antimicrobial loaded filter disks were overlaid. Alternatively, when assessing zones of clearing using M9 minimal medium agar, strains were washed three times in phosphate buffered saline (PBS) and diluted to OD_{600} = 0.1 in fresh PBS. Tested antimicrobials were pentamidine isethionate, chlorhexidine dihydrochloride and 4',6-diamidino-2-phenylindole dihydrochloride (DAPI) at the final concentrations of 125, 2.5 and 1.6 µg, respectively. After overnight incubation, callipers were used to measure the diffusion distances which were determined as half of the inhibition zone diameter, less the length of the disk. At least three independent experiments in duplicate were undertaken. Statistical significance was determined using the Student's *t*-test (two-tailed, unpaired) and *P* values <0.0005 were considered significant.

For plate dilution assays, strains were grown to mid-log phase in MH broth, washed three times in PBS and diluted to OD_{600} = 0.1 in fresh PBS. Serial dilutions (10-fold) were prepared of which 5 µl was spotted onto M9 minimal or MH agar containing various concentrations of pentamidine (32, 64, 128, 256 and 512 mg/L) and growth assessed after overnight incubation at 37°C. To test the effect of growth of different carbon sources, M9 minimal media was supplemented with 0.4% (w/v) of succinic, fumaric, citric, α-ketoglutaric or oxaloacetic acids.

Construction of *A. baumannii* ATCC 17978 deletion strains and genetic complementation

Two methods were adopted to generate specific gene deletions in *A. baumannii* ATCC 17978. The first method used to generate Δ*adeRS* utilized a *sacB*-based strategy [26], where genetic sequence flanking the region of interest and the ERY resistance cassette from pVA891 [27] were PCR amplified, purified and subsequently cloned into a modified pBluescript SK^+ II vector that had the *Bam*HI site removed by end-filling, generating pBl_*adeRS*. Confirmed clones were re-cloned into *Xba*I-digested pEX18Tc [28]. The resulting pEX18Tc_*adeRS* vector was introduced into ATCC 17978 cells via electroporation, as previously described [29]. Transformants were selected on LB agar supplemented with ERY. Counter-selection was undertaken on M9 minimal agar containing ERY and 5% sucrose. The second method used to generate Δ*adeA*, Δ*adeB* and Δ*adeAB* strains utilized the RecET recombinase system with modifications [30]. Briefly, 400-600 bp of sequence flanking the gene(s) were used as templates in a nested overlap extension PCR with the ERY resistance cassette from pVA891 [27]. Approximately, 3.5-

5 µg of the purified linear PCR product was electroporated into ATCC 17978 cells harboring the vector pAT04 and recovered as previously described [30]. Recombinants were selected on LB agar supplemented with ERY. All mutants generated in this study were confirmed by PCR amplification and Sanger sequencing. Primers utilized to generate mutant strains are listed in S2 Table.

For genetic complementation of mutant strains, WT copies of *adeRS* and *adeAB* were cloned into pWH1266 [31] where transcription was driven by the tetracycline promoter. Resulting plasmids denoted pWH::*adeRS* and pWH::*adeAB*, respectively were confirmed by Sanger sequencing. The GEN resistance cassette from pUCGM [32] was PCR amplified and cloned into *Bam*HI digested pWH::*adeAB* generating pWHgent::*adeAB* thus abrogating transcription from the pWH1266 tetracycline promoter. Plasmids were introduced into appropriate *A. baumannii* cells as previously described [33]. Primers used to generate complementation vectors are listed in S2 Table.

Cell treatments and RNA isolation

RNA was isolated from WT and Δ*adeRS* cells and Hiseq RNA transcriptome analysis performed following methodologies as outlined previously [34].

For pentamidine stress assays, WT and Δ*adeRS* strains were grown overnight in MH broth, sub-cultured 1:100 in fresh medium and grown to OD_{600} = 0.6; they were subsequently split into two 10 mL cultures. One 10 mL sample was treated with 7.8 mg/L of pentamidine (0.5 × MIC for Δ*adeRS*), whilst the other remained untreated. Cultures were grown for an additional 30 min before total RNA was extracted as outlined previously [34].

Bioinformatic analysis

Bioinformatic analysis of RNA-seq data was undertaken as described previously [34], with the modification that obtained reads were mapped to the recently re-sequenced *A. baumannii* ATCC 17978 genome (GenBank: CP012004). RNA-seq data have been deposited in the gene expression omnibus database, accession number GSE102711 (https://www.ncbi.nlm.nih.gov/geo/query/acc.cgi?acc=GSE102711).

Quantitative Real-Time PCR

Pentamidine stress and RNA-seq validation experiments were achieved using a two-step qRT-PCR method. RNA samples were first purified as previously described [34], subsequently DNaseI treated (Promega) and then converted to cDNA using an iScript™ cDNA synthesis kit (Biorad), following the manufacturer's instructions. The cDNA generated was used as a template for qRT-PCR using the SYBR® Green JumpStart™ Taq readymix™ (Sigma) in a 20 µl final volume. Either a Rotor-Gene Q (Qiagen, Australia) or RG-3000 (Corbett Life Science, Australia) instrument was used for quantification of cDNA using the following protocol; 1 min at 95°C, followed by 40 cycles of 10 sec at 95°C, 15 sec at 57°C and 20 sec at 72°C. Melt curve analyses were undertaken to ensure only the desired amplicon was generated. Primers used (S2 Table) for amplification of cDNA transcripts were designed using NetPrimer (www.premiersoft.com). Transcriptional levels for RNA-seq validation experiments were corrected to *GAPDH* levels prior to normalization to the ATCC 17978 WT. For pentamidine stress experiments, transcriptional levels of *adeA* were corrected to 16S rDNA levels prior to being normalized to their respective untreated *A. baumannii* cultures. Transcriptional

variations were calculated using the $2^{-\Delta\Delta CT}$ method [35]. Results for pentamidine stress experiments display the mean Log_2 fold change (± SEM) of three biological replicates each undertaken in triplicate. Statistical analyses were performed by Student's *t*-test, two-tailed, unpaired; ** = P <0.01 and *** = P <0.001.

Phenotypic microarray analysis

A. baumannii Δ*adeRS* cells were cultured on LB agar overnight at 37°C. A suspension of cells was made from a single colony in Biolog IF-0 inoculation fluid (Biolog, Inc.) to 85% transmittance and was subsequently diluted 1:200 in Biolog IF-0 containing dye A (Biolog, Inc.) and 0, 8, 16, 32 or 64 mg/L pentamidine. One hundred µL of each dilution was added to each well of the Biolog PM01 and PM02A MicroPlates and placed in an Omnilog automatic plate reader (Biolog, Inc.) for 72 h at 37°C. Color formation from the redox active dye (Biolog dye A) was monitored every 15 min. Data obtained from respiration of Δ*adeRS* under different pentamidine conditions were individually overlaid against the untreated control using the OmniLog File Management/Kinetic Analysis software v1.20.02, and analyzed using OmniLog Parametric Analysis software v1.20.02 (Biolog, Inc.).

Results

Generation of Δ*adeRS* and complemented strains

The *adeRS* operon of *A. baumannii* ATCC 17978 was disrupted through the introduction of an ERY resistance cassette to produce a Δ*adeRS* strain. Complementation of Δ*adeRS* was achieved via reintroduction of a WT copy of *adeRS in trans* on the pWH1266 shuttle

vector, generating Δ*adeRS* pWH::*adeRS* and comparisons were made to cells carrying the empty vector control (Δ*adeRS* pWH1266). To ensure deletion of *adeRS* did not affect viability, growth was monitored by OD_{600} readings in MH broth over an 8 h period; results identified no significant perturbations in the growth rate in laboratory media compared to WT cells (data not shown).

Transcriptomic profiling of Δ*adeRS*

Transcriptome profiling by RNA-sequencing (RNA-seq) of RNA isolated from Δ*adeRS* compared to that from WT ATCC 17978 identified 290 differentially expressed (≥ 2-fold) genes; 210 up-regulated and 80 down-regulated (Fig 1 and S3 Table). RNA-seq results were confirmed by quantitative Real-Time PCR (qRT-PCR) for nine genes that displayed different levels of expression in Δ*adeRS* compared to WT; a good correlation between methods was observed (S1 Fig).

Fig 1. Global transcriptomic response differences of *A. baumannii* ATCC 17978 after deletion of *adeRS*. Each diamond marker represents a predicted gene within the genome ordered according to locus tag along the X-axis and differential expression of WT against Δ*adeRS* are displayed on the Y-axis (Log_2). Positive and negative Log_2-values correlate to up- and down-regulated genes, respectively. Green and red circles highlight genes/gene clusters of interest that have been up- and down-regulated, respectively. See S3 Table for the full list of genes that were differentially expressed ≥ 1 Log_2 fold.

Expression of a number of efflux proteins was affected by inactivation of *adeRS*. For example, the *craA* major facilitator superfamily transporter (ACX60_01760) shown to confer resistance to chloramphenicol and recently chlorhexidine efflux [36] was the highest up-regulated gene (7.1-fold; Fig 1) and *adeA* (ACX60_09125), *adeB* (ACX60_09130) and *aceI* (ACX60_07275) which encode the AdeAB and the AceI efflux pumps, were up-regulated by 2.5, 1.43, and 2-fold, respectively, following deletion of *adeRS*.

Expression of multiple genes involved in virulence were down-regulated in the Δ*adeRS* strain, including the type 1 pilus operon *csuA/BABCDE* (ACX60_06480-06505) (3.2- to 2-fold) and the siderophore-mediated iron-acquisition systems acinetobactin (ACX60_05590-05680) and siderophore 1 (ACX60_09665-09720) clusters (7.7- to 1.1-fold and 5.4- to 0.3-fold, respectively). In contrast, the ferric uptake regulator gene (*fur*) (ACX60_13910) was up-regulated 2.4-fold. Despite these alterations in expression levels of iron siderophore clusters and their regulator, no significant growth defects were identified when Δ*adeRS* was grown in the presence of 200 μM of DIP (data not shown).

Deletion of *adeRS* in ATCC 17978 reduced susceptibility to a limited number of antimicrobial agents

To assess if changes in expression of the *adeAB* and *craA* drug efflux genes identified in the transcriptome of the Δ*adeRS* derivative translated to an alteration in resistance profile, antibiogram analyses were undertaken. Resistance to a number of antibiotics including those that are known substrates of the CraA and AdeABC pumps were assessed. Surprisingly, despite *craA* being the highest up-regulated gene, no change in resistance to

the primary substrate of CraA, chloramphenicol [36], was seen (data not shown). Previous studies examining the level of antimicrobial resistance conferred by AdeABC indicate that only when deletions are generated in strains which overexpress AdeABC is there a significant impact on the antibiogram [10, 13, 15, 16, 37], implying that AdeABC confers only minimal to no intrinsic resistance. This was supported in our analysis as the MIC for tetracycline, tigecycline, GEN, kanamycin, nalidixic acid, ampicillin, streptomycin and amikacin, all previously identified AdeABC substrates, remained unchanged, whilst resistance to norfloxacin and ciprofloxacin increased 2-fold (data not shown) and chlorhexidine decreased 2-fold for the Δ*adeRS* mutant compared to WT (Table 1).

Table 1. Antibiotic susceptibility of *A. baumannii* ATCC 17978, deletion mutants and complemented strains.

	MIC (mg/L)[ab]		
Strain	**PENT**	**DAPI**	**CHX**
WT	125	4	8
Δ*adeRS*	**15.6**	**1**	**4**
Δ*adeAB*	**15.6**	**1**	**4**
Δ*adeA*	**15.6**	**1**	**4**
Δ*adeB*	**15.6**	**1**	**4**
Δ*adeRS* pWH::*adeRS*	125	1	8
Δ*adeRS* pWH1266	15.6	0.5	4/2
Δ*adeRS* pWH::*adeAB*	31.3	4	4
Δ*adeRS* pWHgent::*adeAB*	15.6	1	4
Δ*adeRS* pWHgent	7.8	0.5	4

Δ*adeA* pWHgent::*adeAB*	62.5	2	8/4
Δ*adeA* pWHgent	7.8	0.5	4
Δ*adeB* pWHgent::*adeAB*	62.5	4	4
Δ*adeB* pWHgent	7.8	1	2
Δ*adeAB* pWHgent::*adeAB*	62.5	4	4
Δ*adeAB* pWHgent	7.8	1	2

[a]PENT, pentamidine; DAPI, 4',6-diamidino-2-phenylindole; CHX, chlorhexidine.

[b]Values highlighted in bold indicate MIC values altered two-fold or greater compared to WT ATCC 17978.

Other compounds tested included; colistin, polymyxin B, rifampicin, triclosan, novobiocin, benzalkonium, methyl viologen, pentamidine, DAPI and dequalinium. Of these, significant differences in the MICs of Δ*adeRS* versus WT were observed only for the diamidine compounds, pentamidine and DAPI, where an 8- and 4-fold reduction in resistance was identified, respectively (Table 1). Thus, taken together the Δ*adeRS* strain showed reduced resistance to the bisbiguanide chlorhexidine, and the diamidines pentamidine and DAPI which display structural similarities [38] (S2 Fig). Resistance to these substrates was partially or fully restored by complementation using Δ*adeRS* pWH::*adeRS* (Table 1).

Both AdeA and AdeB are required for intrinsic antimicrobial resistance in ATCC 17978

Since the 10-bp direct repeat where AdeR has been demonstrated to bind in other *A. baumannii* strains [18, 19] is also present in the ATCC 17978 *adeA-adeR* intercistronic region (data not shown), we hypothesized that the decreased resistance towards the

subgroup of dicationic compounds seen in Δ*adeRS* resulted from changes in *adeAB* expression. To test this, deletion strains targeting *adeAB,* as well as individual *adeA* and *adeB* mutations were generated in ATCC 17978.

Using Δ*adeAB*, MIC analyses verified that deletion of the pump resulted in negligible changes in resistance to a subset of the antimicrobials tested for Δ*adeRS* (data not shown). However, an identical resistance pattern for the dicationic compounds as that afforded by Δ*adeRS* was observed (Table 1). Complementation of the inactivated genes partially restored resistance to all compounds, validating that AdeAB plays a direct role in resistance to these dicationic compounds (Table 1).

AdeRS is critical for increased expression of *adeAB* following pentamidine exposure

From MIC analysis of the ATCC 17978 derivatives, it was proposed that the presence of the AdeRS TCSTS increased *adeAB* expression consequently providing resistance to pentamidine, chlorhexidine and DAPI (Table 1). To confirm this, the level of *adeA* transcription was assessed by qRT-PCR of RNA isolated from WT and Δ*adeRS* strains after addition of a sub-inhibitory concentration of pentamidine. Transcription of the *adeAB* operon was significantly up-regulated in WT and down-regulated in Δ*adeRS* following pentamidine stress (Fig 2). Additionally, qRT-PCR was used to determine if *adeS* expression levels altered after pentamidine stress in WT cells. It was found that *adeS* expression increased less than <2-fold compared to untreated WT cells (data not shown). To phenotypically support the transcriptional evidence that *adeRS* initiates transcription of the ATCC 17978 *adeAB* operon, additional antibiograms were

determined. Using the shuttle vector pWH1266, two clones were constructed; pWH::*adeAB* and pWHgent::*adeAB*, where the GEN resistance cartridge cloned in the latter vector inhibited transcription of *adeAB* from the tetracycline promoter naturally present in pWH1266. MIC analyses determined that the carriage of pWHgent::*adeAB* in Δ*adeRS* did not differ from results obtained for Δ*adeRS*. Conversely, Δ*adeRS* cells with pWH::*adeAB* displayed a 4- and 8-fold increase in pentamidine and DAPI resistance, respectively (Table 1). Collectively, these results suggest that expression of *adeAB* and subsequent resistance to the dicationic compounds in ATCC 17978 can only occur when AdeRS is present.

Fig 2. Increased expression of *adeA* following pentamidine stress is dependent on the presence of AdeRS in ATCC 17978. Transcriptional levels of *adeA* (ACX60_09125) from WT and Δ*adeRS* were determined by qRT-PCR after 30 min shock with 7.8 mg/L of pentamidine (Pent) (0.5 × MIC of Δ*adeRS*) and corrected to untreated cells (UT) after normalization to 16S. Bars represent the mean fold change (Log_2) of three biological replicates undertaken in triplicate, and error bars represent ± SEM. Statistical analyses were performed by Student's *t*-test, two-tailed, unpaired; ** = $P < 0.01$ and *** = $P < 0.001$.

Carbon source utilization alters resistance to pentamidine

Pentamidine, a drug known to be effective in the treatment of fungal and protozoan infections has gained recent attention in a bacterial context. Pentamidine has shown

328 synergy with Gram-positive antibiotics, potentiating their activity towards Gram-negative
329 bacteria [23]. As such, pentamidine has been proposed to be utilized as an adjunct therapy
330 for MDR bacteria, including *A. baumannii* [23]. To identify additional pentamidine
331 resistance mechanisms employed by *A. baumannii*, growth in different media was
332 assessed. Disk diffusion assays identified that in *A. baumannii*, resistance to pentamidine
333 was affected by the carbon source provided in M9 minimal medium (S4 Table), whilst for
334 chlorhexidine and DAPI this pattern was not conserved indicating a pentamidine-specific
335 response (data not shown). To determine the MIC levels for pentamidine, plate dilution
336 experiments were undertaken for WT, Δ*adeRS* and Δ*adeAB* strains provided with varied
337 carbon sources (Fig 3). Growth of Δ*adeRS* and Δ*adeAB* cells on MH agar were
338 significantly perturbed at 32 mg/L of pentamidine. This MIC drastically differs when
339 succinic acid was utilized as the sole carbon source, as growth was maintained up to 512
340 mg/L of pentamidine for all strains tested (Fig 3). Fumaric, α-ketoglutaric and
341 oxaloacetic acids also increased pentamidine resistance by 8-fold for Δ*adeRS* and
342 Δ*adeAB* strains when compared to the MIC obtained for MH agar. Growth of Δ*adeRS*
343 and Δ*adeAB* mutants was inhibited at a higher dilution factor in the presence of
344 oxaloacetic acid compared to fumaric and α-ketoglutaric acids whilst growth using citrate
345 as the sole carbon source negatively affected resistance to WT cells, decreasing resistance
346 2-fold.

347 **Fig 3. Resistance to pentamidine is modulated by carbon sources available in the**
348 **growth medium.** Ten-fold serial dilutions of *A. baumannii* ATCC 17978 (WT), Δ*adeRS*
349 (Δ*RS*) and Δ*adeAB* (Δ*AB*) cells were used to compare the concentration of pentamidine
350 that inhibits growth in different media, Mueller-Hinton agar (MHA) was used as a

351 comparative control. Images display serial 1:10 dilutions after overnight incubation at
352 37°C, where DF is abbreviated for dilution factor and N represents undiluted cells.
353 Strains were grown in the absence of pentamidine (UT) or presence of 32, 64, 128, 256
354 and 512 mg/L of pentamidine (P32, P64, P128, P256, and P512, respectively). Carbon
355 sources tested in M9 minimal medium were used at a final concentration of 0.4% (w/v).
356 ND, not done due to precipitation of pentamidine once added into the molten medium.
357 Figures are representative examples of results obtained.

358 Biolog phenotypic arrays were undertaken to identify additional synergistic or
359 antagonistic relationships between carbon sources and pentamidine resistance.
360 Respiration of Δ*adeRS* cells for a total of 190 carbon compounds was assessed at various
361 pentamidine concentrations (S3 Fig). From this, an additional ten compounds were
362 identified that increased resistance to pentamidine in Δ*adeRS* at 64 mg/L (Fig 4). Despite
363 minimal changes in pentamidine resistance in the presence of citric acid for Δ*adeRS* (Fig
364 3), this compound negatively affected respiration at lower pentamidine concentrations
365 (S3 Fig). Surprisingly, succinic, α-ketoglutaric and fumaric acids failed to restore
366 respiration at 64 mg/L of pentamidine for Δ*adeRS* (S3 Fig). By extending the incubation
367 period for another 72 h, respiration in the presence of succinic or fumaric acids was
368 restored to levels similar to the untreated control (data not shown). This may indicate that
369 succinic and fumaric acids significantly lag in their ability to recover the cells from
370 pentamidine in the IF-0 medium (Biolog Inc.) whilst α-ketoglutaric acid recovery is
371 dependent on growth medium.

Fig 4. Kinetic response curves paralleling bacterial growth from Biolog PM01 and PM2A plates identify ten carbon sources that increase pentamidine resistance in Δ*adeRS*. P8, P16, P32 and P64 represent kinetic response curves at 8, 16, 32, or 64 mg/L of pentamidine compared to the untreated control, respectively. Red curves represent respiration of untreated Δ*adeRS*, whilst respiratory activity which overlaps between the control and the sample in the different experimental conditions is represented in yellow. Only carbon compounds that promote at least 50% maximal respiration and induce a recovery response by 36 h are shown. See S3 Fig for respiration curves for all tested treatments.

Bioavailability of iron correlates with pentamidine resistance

Iron has been shown to influence pentamidine resistance in protozoan species [39], thus we assessed if its plays a similar role in *A. baumannii*. The addition of ferrous sulphate to the growth medium significantly reduced the zone of clearing from pentamidine in a dose-dependent manner up to a final concentration of 5 mM for WT and mutant strains (Table 2 and S4 Fig). Furthermore, chelation of iron using DIP resulted in WT cells becoming more susceptible to pentamidine compared to the untreated control (Table 2). This modified pentamidine susceptibility is iron specific as inclusion of other cations in the growth medium (zinc, copper, manganese, cobalt, nickel) did not significantly affect the zones of clearing (data not shown). Using inductively-coupled plasma mass spectrometry the internal iron concentration in WT and Δ*adeRS* cells was determined in the absence/presence of a sub-inhibitory concentration of pentamidine. Internal iron

concentrations remained essentially unchanged in both strains under the different conditions tested (data not shown), indicating that iron/pentamidine interactions may occur outside of the cell and the observed response was not due to a reduced capacity to store iron.

Table 2. Zones of clearing for *A. baumannii* ATCC 17978 and deletion mutants grown on Mueller-Hinton agar with the addition or chelation of iron after pentamidine exposure.

	Zone of clearing (mm)[ab]				
Strain	**WT**	**Δ*adeRS***	**Δ*adeAB***	**Δ*adeA***	**Δ*adeB***
Medium[c]					
MHA control	1.4 ± 0.3	6.9 ± 0.5	6.9 ± 0.3	6.9 ± 0.4	7.2 ± 0.4
+ 2.5 mM $FeSO_4$	**0.8 ± 0.1***	**5.4 ± 0.2***	**5.6 ± 0.3***	**5.4 ± 0.1*****	**5.6 ± 0.1*****
+ 5 mM $FeSO_4$	**0.7 ± 0.2***	**2.5 ± 0.8*****	**2.8 ± 0.3*****	**3.2 ± 0.3*****	**2.9 ± 0.6*****
+ 7.5 mM $FeSO_4$	NG	NG	NG	NG	NG
+ 100 µM DIP	1.7 ± 0.1	6.7 ± 0.2	6.9 ± 0.1	6.2 ± 0.2	6.6 ± 0.2
+ 200 µM DIP	**5 ± 0.3*****	6.7 ± 0.4	6.6 ± 0.4	6.1 ± 0.1	6.4 ± 0.1

[a]Averaged values are displayed ± SD. Statistical analyses were performed by Student's *t*-test, two-tailed, unpaired; * = P <0.0005 and *** = P <0.000001.

[b]Values given in bold indicate a significant difference between a strain grown under iron-rich or iron-limited conditions versus its respective MHA control.

[c]MHA, Mueller-Hinton agar; $FeSO_4$, ferrous sulphate; DIP, 2',2' dipyridyl; NG, no growth due to iron toxicity.

Discussion

409 The *adeRS* and *adeABC* operons of *A. baumannii* have gained considerable attention due
410 to their role in regulating and conferring multidrug resistance, respectively [8, 13, 16, 40].
411 Multiple genetic arrangements of the *adeABC* operon in *A. baumannii* clinical isolates
412 exist, where 35% of 116 diverse isolates lack the *adeC* OMP component [20]. This is also
413 the case for the clinical isolate *A. baumannii* ATCC 17978, which was chosen for further
414 analysis in this study. It is not uncommon for RND pumps to recruit an alternative OMP
415 to form a functional complex [41-43]. This may also be the situation for AdeAB in *A.*
416 *baumannii* ATCC 17978, since in an *Escherichia coli* background, *adeAB* can be co-
417 expressed with *adeK*, an OMP belonging to the *A. baumannii* AdeIJK RND complex to
418 confer resistance [44]. However, whether AdeB can work alone or function with
419 alternative membrane fusion proteins such as *adeI* or *adeF* is not known. As the
420 resistance profile of Δ*adeA* was indistinguishable from the Δ*adeAB* and Δ*adeB* strains, it
421 provides confirmatory evidence that both *adeA* and *adeB* are required for efficient efflux
422 to only a subset of dicationic compounds in ATCC 17978. Further assessments will be
423 required to verify if this phenotype is maintained across other *A. baumannii* isolates and
424 extends to other structurally-similar compounds.

425 It has been found previously, that the introduction of shuttle vectors expressing WT
426 copies of genes *in trans* do not restore resistance profiles back to WT levels as also seen
427 in this study [45-48]. Using qRT-PCR, *adeS* was expressed at low levels in WT cells
428 even after pentamidine shock (data not shown). Complementation studies with *adeRS*
429 thus could be influenced by copy number effects, which may perturb the native
430 expression levels of these proteins within the cell. Additionally, the differing modes of
431 action of the dicationic compounds may have influenced the MIC results, as fold-shifts in

resistance were observed even when the empty pWH1266 vector was being expressed (Table 1).

The transcriptomic analysis of ATCC 17978 Δ*adeRS* revealed changes in gene expression were not limited to *adeAB* but included many genes, some of which have been shown to be important in *A. baumannii* pathogenesis [49, 50] and virulence *in vivo* [51]. Although this had been seen before in an *adeRS* mutant generated in the MDR *A. baumannii* isolate AYE [16], here the transcriptional changes were to a largely different subset of genes. In particular, deletion of *adeRS* in AYE resulted in decreased expression of *adeABC* by 128-, 91-, and 28-fold, respectively [16]. This decreased gene expression was expected as AYE naturally contains a point mutation in AdeS (producing an Ala 94 to Val substitution in AdeS) resulting in constitutive expression of *adeABC*, thus contributing to its MDR phenotype [2, 16]. Conversely, our transcriptome data indicated that *adeAB* is only expressed at low levels in WT ATCC 17978, a strain labelled as having a 'drug susceptible' phenotype [24].

Currently, the environmental signal(s) that interact with the periplasmic sensing domain of AdeS are not known. Antimicrobial compounds can directly stimulate autophosphorylation of specific TCSTS which in turn directly regulate the expression of genes providing resistance to that compound [52, 53]. It is unlikely that pentamidine is the environmental stimulus that is sensed by AdeS, as a number of conditions, including chlorhexidine shock, can also up-regulate *adeAB* expression in ATCC 17978 [54-57]. Instead, AdeS may respond to stimuli such as solutes that are excreted and accumulate in the periplasm when cells are subjected to various stressors including AdeAB substrates.

This study revealed unique interactions between pentamidine and a number of carbon sources which significantly alter the resistance profile to pentamidine for *A.*

456 *baumannii* ATCC 17978 and derivatives. Biolog phenotypic arrays identified a number of
457 succinic acid derivatives that also allowed respiration in the presence of a lethal
458 concentration of pentamidine (Fig 4). Interestingly, when Δ*adeRS* utilized malonic acid
459 as the sole carbon source, a potent inhibitor of the succinate dehydrogenase complex,
460 cells were also able to respire at increased pentamidine concentrations (Fig 4). In Gram-
461 negative bacteria, the mechanism of action for pentamidine is thought to primarily occur
462 via binding to the lipid-A component of the outer membrane and not through inhibition of
463 an intracellular target [23, 58]. Therefore, it seems unlikely that pentamidine interferes
464 with enzymatic functions like that of succinate dehydrogenase, and instead the
465 compounds which showed an increase in pentamidine resistance may contribute to either
466 chelation of the compound or provide protective mechanisms that reduce binding to the
467 lipid-A target. Interestingly, a 1956 study [59] identified that in the presence of α-
468 ketoglutaric or glutamic acid, resistance to a lethal concentration of pentamidine could be
469 achieved in *E. coli*, leading to the proposition that pentamidine interferes with the
470 transaminase reaction in glutamic acid production. However, our study shows that
471 glutamic acid does not affect pentamidine resistance (S4 Table), inferring that a different
472 mechanism might be responsible for the increase in pentamidine resistance in *A.*
473 *baumannii*.

474 Iron is an essential metal serving as a co-factor in numerous proteins involved in
475 redox chemistry and electron transport. It is generally a limited resource for pathogenic
476 bacteria such as *A. baumannii* where it is important for virulence and disease progression
477 [6, 50]. Our studies showed that altering iron levels also had a marked effect on resistance
478 to pentamidine. This is in agreement with the observation that citric and gluconic acids

can act as iron-chelating agents [60, 61] and respiration activity in the presence of these compounds at the pentamidine concentrations tested were significantly altered (S3 Fig). Many clinically relevant antimicrobials have shown to be affected by the presence of iron, including compounds belonging to tetracycline, aminoglycoside and quinolone classes [22]. Activity of these compounds can be altered by numerous factors, including the formation of stable complexes which can affect drug efficacy or have unfavourable effects on patient health.

Conclusions

Overall, this is the first study which has demonstrated that the AdeAB system in *A. baumannii* ATCC 17978 provides intrinsic resistance to a subset of dicationic compounds, and efflux of these compounds via AdeAB is directly regulated by the AdeRS TCSTS. RNA-seq identified that deletion of *adeRS* produced significant changes in the transcriptome where our results support the notion that strain specific variations are apparent [16]. We have provided evidence that in ATCC 17978, AdeRS is directly responsible for the activation of *adeAB* gene expression, as Δ*adeRS* failed to increase expression upon subjection to one of the pumps newly identified intrinsic substrates, pentamidine. It will be of interest to assess whether these dicationic compounds also extend as substrates towards AdeAB(C) pumps present in other *A. baumannii* isolates and if expression levels of *adeAB(C)* upon exposure to these substrates and other potential stressors also occur. This information may help to identify the stimulus that activates the AdeRS TCSTS. We have also demonstrated for the first time that for pentamidine to exert its antibacterial effect in *A. baumannii*, a dependence on the availability of iron is

501 required, and that growth in the presence of selected carbon sources has a profound effect
502 on its resistance.

503 Acknowledgments

504 We would like to thank Professor Bryan Davies from the Department of Molecular
505 Biosciences at the University of Texas for providing the plasmid pAT04.

506 References

507 1. Peleg AY, Seifert H, Paterson DL. *Acinetobacter baumannii*: emergence of a
508 successful pathogen. Clin Microbiol Rev. 2008;21(3):538-82.
509 2. Fournier PE, Vallenet D, Barbe V, Audic S, Ogata H, Poirel L, et al. Comparative
510 genomics of multidrug resistance in *Acinetobacter baumannii*. PLoS Genet.
511 2006;2(1):e7.
512 3. Adams MD, Chan ER, Molyneaux ND, Bonomo RA. Genomewide analysis of
513 divergence of antibiotic resistance determinants in closely related isolates of
514 *Acinetobacter baumannii*. Antimicrob Agents Chemother. 2010;54(9):3569-77.
515 4. Blackwell GA, Hamidian M, Hall RM. IncM plasmid R1215 is the source of
516 chromosomally located regions containing multiple antibiotic resistance genes in
517 the globally disseminated *Acinetobacter baumannii* GC1 and GC2 clones. mSphere.
518 2016;1(3):e00117-16.
519 5. Hamidian M, Kenyon JJ, Holt KE, Pickard D, Hall RM. A conjugative plasmid
520 carrying the carbapenem resistance gene *bla*OXA-23 in AbaR4 in an extensively

resistant GC1 *Acinetobacter baumannii* isolate. J Antimicrob Chemother. 2014;69(10):2625-8.

6. Wright MS, Jacobs MR, Bonomo RA, Adams MD. Transcriptome remodeling of *Acinetobacter baumannii* during infection and treatment. MBio. 2017;8(2):e02193-16.

7. Saranathan R, Pagal S, Sawant AR, Tomar A, Madhangi M, Sah S, et al. Disruption of TetR type regulator *adeN* by mobile genetic element confers elevated virulence in *Acinetobacter baumannii*. Virulence. 2017:1-19.

8. Yoon EJ, Courvalin P, Grillot-Courvalin C. RND-type efflux pumps in multidrug-resistant clinical isolates of *Acinetobacter baumannii*: major role for AdeABC overexpression and AdeRS mutations. Antimicrob Agents Chemother. 2013;57(7):2989-95.

9. Coyne S, Courvalin P, Perichon B. Efflux-mediated antibiotic resistance in *Acinetobacter* spp. Antimicrob Agents Chemother. 2011;55(3):947-53.

10. Magnet S, Courvalin P, Lambert T. Resistance-nodulation-cell division-type efflux pump involved in aminoglycoside resistance in *Acinetobacter baumannii* strain BM4454. Antimicrob Agents Chemother. 2001;45(12):3375-80.

11. Coyne S, Rosenfeld N, Lambert T, Courvalin P, Perichon B. Overexpression of resistance-nodulation-cell division pump AdeFGH confers multidrug resistance in *Acinetobacter baumannii*. Antimicrob Agents Chemother. 2010;54(10):4389-93.

12. Damier-Piolle L, Magnet S, Bremont S, Lambert T, Courvalin P. AdeIJK, a resistance-nodulation-cell division pump effluxing multiple antibiotics in *Acinetobacter baumannii*. Antimicrob Agents Chemother. 2008;52(2):557-62.

13. Marchand I, Damier-Piolle L, Courvalin P, Lambert T. Expression of the RND-type efflux pump AdeABC in *Acinetobacter baumannii* is regulated by the AdeRS two-component system. Antimicrob Agents Chemother. 2004;48(9):3298-304.

14. Peleg AY, Adams J, Paterson DL. Tigecycline efflux as a mechanism for nonsusceptibility in *Acinetobacter baumannii*. Antimicrob Agents Chemother. 2007;51(6):2065-9.

15. Rajamohan G, Srinivasan VB, Gebreyes WA. Novel role of *Acinetobacter baumannii* RND efflux transporters in mediating decreased susceptibility to biocides. J Antimicrob Chemother. 2010;65(2):228-32.

16. Richmond GE, Evans LP, Anderson MJ, Wand ME, Bonney LC, Ivens A, et al. The *Acinetobacter baumannii* two-component system AdeRS regulates genes required for multidrug efflux, biofilm formation, and virulence in a strain-specific manner. MBio. 2016;7(2):e00430-16.

17. Nikaido H, Takatsuka Y. Mechanisms of RND multidrug efflux pumps. Biochim Biophys Acta. 2009;1794(5):769-81.

18. Chang TY, Huang BJ, Sun JR, Perng CL, Chan MC, Yu CP, et al. AdeR protein regulates *adeABC* expression by binding to a direct-repeat motif in the intercistronic spacer. Microbiol Res. 2016;183:60-7.

19. Wen YO, Z., Yu Y, Zhou X, Pei YD, B., Higgins P, Zheng F. Mechanistic insight into how multidrug resistant *Acinetobacter baumannii* response regulator AdeR recognizes an intercistronic region Nucleic Acids Res. 2017;45(16):9773-87.

20. Nemec A, Maixnerova M, van der Reijden TJ, van den Broek PJ, Dijkshoorn L. Relationship between the AdeABC efflux system gene content, netilmicin

susceptibility and multidrug resistance in a genotypically diverse collection of *Acinetobacter baumannii* strains. J Antimicrob Chemother. 2007;60(3):483-9.

21. Conrad RS, Wulf RG, Clay DL. Effects of carbon sources on antibiotic resistance in *Pseudomonas aeruginosa*. Antimicrob Agents Chemother. 1979;15(1):59-66.

22. Ezraty B, Barras F. The 'liaisons dangereuses' between iron and antibiotics. FEMS Microbiol Rev. 2016;40(3):418-35.

23. Stokes JM, MacNair CR, Ilyas B, French S, Cote JP, Bouwman C, et al. Pentamidine sensitizes Gram-negative pathogens to antibiotics and overcomes acquired colistin resistance. Nat Microbiol. 2017;2:17028.

24. Smith MG, Gianoulis TA, Pukatzki S, Mekalanos JJ, Ornston LN, Gerstein M, et al. New insights into *Acinetobacter baumannii* pathogenesis revealed by high-density pyrosequencing and transposon mutagenesis. Genes Dev. 2007;21(5):601-14.

25. Wiegand I, Hilpert K, Hancock RE. Agar and broth dilution methods to determine the minimal inhibitory concentration (MIC) of antimicrobial substances. Nat Protoc. 2008;3(2):163-75.

26. Kaniga K, Delor I, Cornelis GR. A wide-host-range suicide vector for improving reverse genetics in Gram-negative bacteria: inactivation of the *blaA* gene of *Yersinia enterocolitica*. Gene. 1991;109(1):137-41.

27. Macrina FL, Evans RP, Tobian JA, Hartley DL, Clewell DB, Jones KR. Novel shuttle plasmid vehicles for *Escherichia-Streptococcus* transgeneric cloning. Gene. 1983;25(1):145-50.

28. Hoang TT, Karkhoff-Schweizer RR, Kutchma AJ, Schweizer HP. A broad-host-range Flp-FRT recombination system for site-specific excision of chromosomally-

591 located DNA sequences: application for isolation of unmarked *Pseudomonas*
592 *aeruginosa* mutants. Gene. 1998;212(1):77-86.
593 29. Dorsey CW, Tomaras AP, Actis LA. Genetic and phenotypic analysis of
594 *Acinetobacter baumannii* insertion derivatives generated with a transposome
595 system. Appl Environ Microbiol. 2002;68(12):6353-60.
596 30. Tucker AT, Nowicki EM, Boll JM, Knauf GA, Burdis NC, Trent MS, et al.
597 Defining gene-phenotype relationships in *Acinetobacter baumannii* through one-
598 step chromosomal gene inactivation. MBio. 2014;5(4):e01313-14.
599 31. Hunger M, Schmucker R, Kishan V, Hillen W. Analysis and nucleotide sequence of
600 an origin of DNA replication in *Acinetobacter calcoaceticus* and its use for
601 *Escherichia coli* shuttle plasmids. Gene. 1990;87(1):45-51.
602 32. Schweizer HD. Small broad-host-range gentamycin resistance gene cassettes for
603 site-specific insertion and deletion mutagenesis. Biotechniques. 1993;15(5):831-4.
604 33. Eijkelkamp BA, Stroeher UH, Hassan KA, Elbourne LD, Paulsen IT, Brown MH.
605 H-NS plays a role in expression of *Acinetobacter baumannii* virulence features.
606 Infect Immun. 2013;81(7):2574-83.
607 34. Giles SK, Stroeher UH, Eijkelkamp BA, Brown MH. Identification of genes
608 essential for pellicle formation in *Acinetobacter baumannii*. BMC Microbiol.
609 2015;15:116.
610 35. Livak KJ, Schmittgen TD. Analysis of relative gene expression data using real-time
611 quantitative PCR and the $2^{(-\Delta\Delta C(T))}$ method. Methods. 2001;25(4):402-8.
612 36. Li L, Hassan KA, Brown MH, Paulsen IT. Rapid multiplexed phenotypic screening
613 identifies drug resistance functions for three novel efflux pumps in *Acinetobacter*
614 *baumannii*. J Antimicrob Chemother. 2016;71(5):1223-32.

615 37. Yoon EJ, Chabane YN, Goussard S, Snesrud E, Courvalin P, De E, et al.
616 Contribution of resistance-nodulation-cell division efflux systems to antibiotic
617 resistance and biofilm formation in *Acinetobacter baumannii*. MBio.
618 2015;6(2):e00309-15.
619 38. Brown MH, Skurray RA. Staphylococcal multidrug efflux protein QacA. J Mol
620 Microbiol Biotechnol. 2001;3(2):163-70.
621 39. Wong IL, Chow LM. The role of *Leishmania enriettii* multidrug resistance protein
622 1 (LeMDR1) in mediating drug resistance is iron-dependent. Mol Biochem
623 Parasitol. 2006;150(2):278-87.
624 40. Nowak J, Schneiders T, Seifert H, Higgins PG. The Asp20-to-Asn substitution in
625 the response regulator AdeR leads to enhanced efflux activity of AdeB in
626 *Acinetobacter baumannii*. Antimicrob Agents Chemother. 2016;60(2):1085-90.
627 41. Chuanchuen R, Narasaki CT, Schweizer HP. The MexJK efflux pump of
628 *Pseudomonas aeruginosa* requires OprM for antibiotic efflux but not for efflux of
629 triclosan. J Bacteriol. 2002;184(18):5036-44.
630 42. Mine T, Morita Y, Kataoka A, Mizushima T, Tsuchiya T. Expression in
631 *Escherichia coli* of a new multidrug efflux pump, MexXY, from *Pseudomonas*
632 *aeruginosa*. Antimicrob Agents Chemother. 1999;43(2):415-7.
633 43. Fralick JA. Evidence that TolC is required for functioning of the Mar/AcrAB efflux
634 pump of *Escherichia coli*. J Bacteriol. 1996;178(19):5803-5.
635 44. Sugawara E, Nikaido H. Properties of AdeABC and AdeIJK efflux systems of
636 *Acinetobacter baumanii* compared with those of AcrAB-TolC system of
637 *Escherichia coli*. Antimicrob Agents Chemother. 2014;58:7250-7.

638 45. Li X, Quan J, Yang Y, Ji J, Liu L, Fu Y, et al. Abrp, a new gene, confers reduced
639 susceptibility to tetracycline, glycylcine, chloramphenicol and fosfomycin classes
640 in *Acinetobacter baumannii*. Eur J Clin Microbiol Infect Dis. 2016;35(8):1371-5.
641 46. Liou ML, Soo PC, Ling SR, Kuo HY, Tang CY, Chang KC. The sensor kinase
642 BfmS mediates virulence in *Acinetobacter baumannii*. J Microbiol Immunol Infect.
643 2014;47(4):275-81.
644 47. Saroj SD, Clemmer KM, Bonomo RA, Rather PN. Novel mechanism for
645 fluoroquinolone resistance in *Acinetobacter baumannii*. Antimicrob Agents
646 Chemother. 2012;56(9):4955-7.
647 48. Wang J, Zhou Z, He F, Ruan Z, Jiang Y, Hua X, et al. The role of the type VI
648 secretion system *vgrG* gene in the virulence and antimicrobial resistance of
649 *Acinetobacter baumannii* ATCC 19606. PLoS One. 2018;13(2):e0192288.
650 49. Tomaras AP, Dorsey CW, Edelmann RE, Actis LA. Attachment to and biofilm
651 formation on abiotic surfaces by *Acinetobacter baumannii*: involvement of a novel
652 chaperone-usher pili assembly system. Microbiology. 2003;149(Pt 12):3473-84.
653 50. Gaddy JA, Arivett BA, McConnell MJ, Lopez-Rojas R, Pachon J, Actis LA. Role
654 of acinetobactin-mediated iron acquisition functions in the interaction of
655 *Acinetobacter baumannii* strain ATCC 19606T with human lung epithelial cells,
656 *Galleria mellonella* caterpillars, and mice. Infect Immun. 2012;80(3):1015-24.
657 51. Murray GL, Tsyganov K, Kostoulias XP, Bulach DM, Powell D, Creek DJ, et al.
658 Global gene expression profile of *Acinetobacter baumannii* during bacteremia. J
659 Infect Dis. 2017;215(suppl_1):S52-7.

660 52. Koteva K, Hong HJ, Wang XD, Nazi I, Hughes D, Naldrett MJ, et al. A
661 vancomycin photoprobe identifies the histidine kinase VanSsc as a vancomycin
662 receptor. Nat Chem Biol. 2010;6(5):327-9.
663 53. Li L, Wang Q, Zhang H, Yang M, Khan MI, Zhou X. Sensor histidine kinase is a β-
664 lactam receptor and induces resistance to β-lactam antibiotics. Proc Natl Acad Sci
665 USA. 2016;113(6):1648-53.
666 54. Hassan KA, Jackson SM, Penesyan A, Patching SG, Tetu SG, Eijkelkamp BA, et
667 al. Transcriptomic and biochemical analyses identify a family of chlorhexidine
668 efflux proteins. Proc Natl Acad Sci USA. 2013;110(50):20254-9.
669 55. Eijkelkamp BA, Hassan KA, Paulsen IT, Brown MH. Investigation of the human
670 pathogen *Acinetobacter baumannii* under iron limiting conditions. BMC Genomics.
671 2011;12:126.
672 56. Lin MF, Lin YY, Lan CY. The role of the two-component system BaeSR in
673 disposing chemicals through regulating transporter systems in *Acinetobacter*
674 *baumannii*. PLoS One. 2015;10(7):e0132843.
675 57. Camarena L, Bruno V, Euskirchen G, Poggio S, Snyder M. Molecular mechanisms
676 of ethanol-induced pathogenesis revealed by RNA-sequencing. PLoS Pathog.
677 2010;6(4):e1000834.
678 58. David SA, Bechtel B, Annaiah C, Mathan VI, Balaram P. Interaction of cationic
679 amphiphilic drugs with lipid A: implications for development of endotoxin
680 antagonists. Biochim Biophys Acta. 1994;1212(2):167-75.
681 59. Amos H, Vollmayer E. Effect of pentamidine on the growth of *Escherichia coli*. J
682 Bacteriol. 1957;73(2):172-7.

683 60. Hamm RE, Shull Jr. CM, Grant DM. Citrate complexes with iron(II) and iron(III). J
684 Am Chem Soc 1953;76:2111-4.
685 61. Pecsok RL, Sandera J. The gluconate complexes. II. The ferric-gluconate system. J
686 Am Chem Soc. 1955;77(6):1489-94.

687

688 Supporting information

689 **S1 Fig. Validation of RNA-sequencing results.** The transcriptomic results obtained by
690 RNA-sequencing were validated by qRT-PCR analysis. The level of nine genes that
691 displayed differential expression or remained essentially unchanged between Δ*adeRS* and
692 WT ATCC 17978 were chosen for comparison. Expression levels for qRT-PCR
693 experiments were corrected to those obtained for *GAPDH* (ACX60_05065) prior to
694 normalisation against WT ATCC 17978 transcriptional levels. Grey and black bars
695 represent values obtained from RNA-seq and qRT-PCR results, respectively. Differential
696 expression between Δ*adeRS* and WT ATCC 17978 are given in Log_2-values.

697 **S2 Fig. Structures of dicationic antimicrobial compounds to which Δ*adeRS*, Δ*adeA*,**
698 **Δ*adeB* and Δ*adeAB* deletion mutant derivatives showed a decrease in resistance**
699 **when compared to WT ATCC 17978.** Compounds include (a) pentamidine, (b) DAPI
700 and (c) chlorhexidine. For pentamidine and chlorhexidine, the cationic nitrogenous
701 groups are separated by a long carbon chain, forming symmetrical compounds, whereas,
702 DAPI lacks this long linker and is asymmetric

703 **S3 Fig. Comparative analysis of kinetic response curves obtained from Biolog PM**
704 **plates for Δ*adeRS* cells untreated and subjected to increasing concentrations of**

pentamidine. Respiration of ATCC 17978 Δ*adeRS* cells in the presence of pentamidine (8, 16, 32, or 64 mg/L) against untreated control cells are shown for (a) Biolog PM01 plates and (b) Biolog PM02A plates. Respiration activity for both plates were monitored in IF-0 (Biolog, Inc.) liquid medium for 72 h at 37°C. The curve in each well represents the colour intensity of a redox-active dye (*y* axis) over time (*x* axis: 72 h). Respiration of Δ*adeRS* cells are shown in red (control), green (under different concentrations of pentamidine), and yellow (depicts the regions of respiratory overlap). Black numbered squares represent carbon sources which decreased resistance to pentamidine (1, D-gluconic acid; 2, citric acid).

S4 Fig. **Pentamidine resistance is affected by the concentration of iron within the growth medium. Resistance to pentamidine was assessed by disc diffusion assays in Mueller-Hinton agar (MHA) for ATCC 17978 and Δ*adeRS*, Δ*adeA*, Δ*adeB* and Δ*adeAB* deletion derivatives.** Zones of clearing were compared to iron rich conditions from the addition of ferrous sulphate ($FeSO_4$) at the final concentrations of 2.5 and 5 mM and iron-chelated conditions obtained by the addition of 2',2' dipyridyl (DIP) at the final concentrations of 100 and 200 μM in MHA. Images displayed are a representative of the typical results obtained.

S1 Table. Strains and plasmids used in the study.

S2 Table. Primers used in this study.

S3 Table. Genes significantly up- and down-regulated (≥ 2-fold) in Δ*adeRS* compared against the parent ATCC 17978 (CP012004) by RNA-seq methodologies.

S4 Table. Zones of clearing obtained from growth on M9 minimal medium with the addition of different carbon sources after exposure to pentamidine.

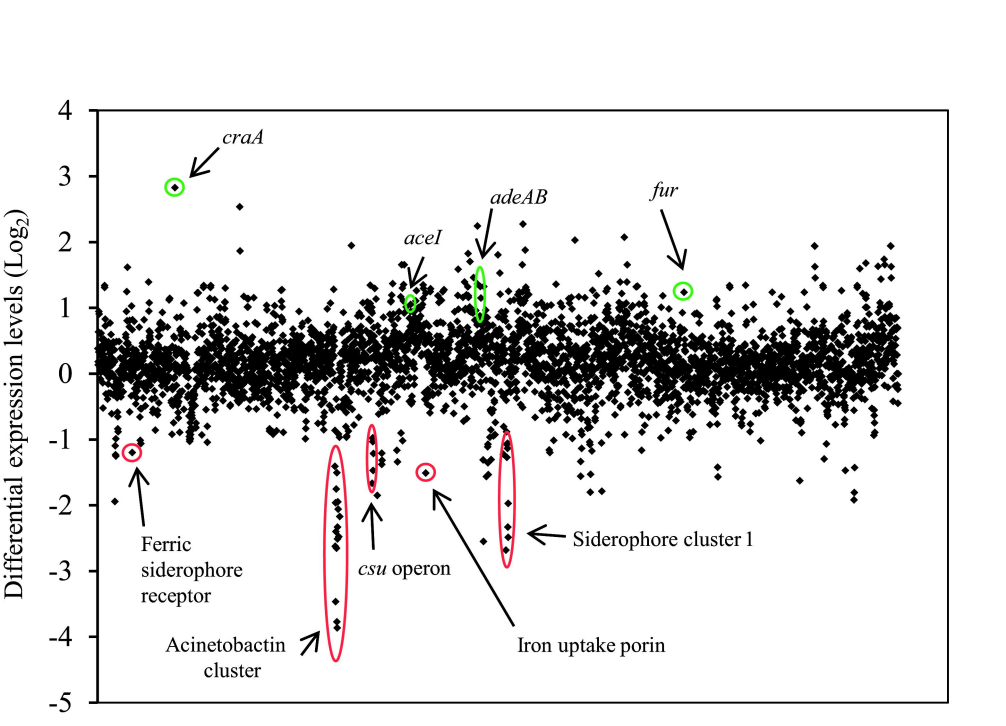
Differential expression levels (Log2)
4
3
2
1
0
-1
-2
-3
-4
-5
craA
aceI
adeAB
fur
Ferric siderophore receptor
Acinetobactin cluster
csu operon
Iron uptake porin
Siderophore cluster 1

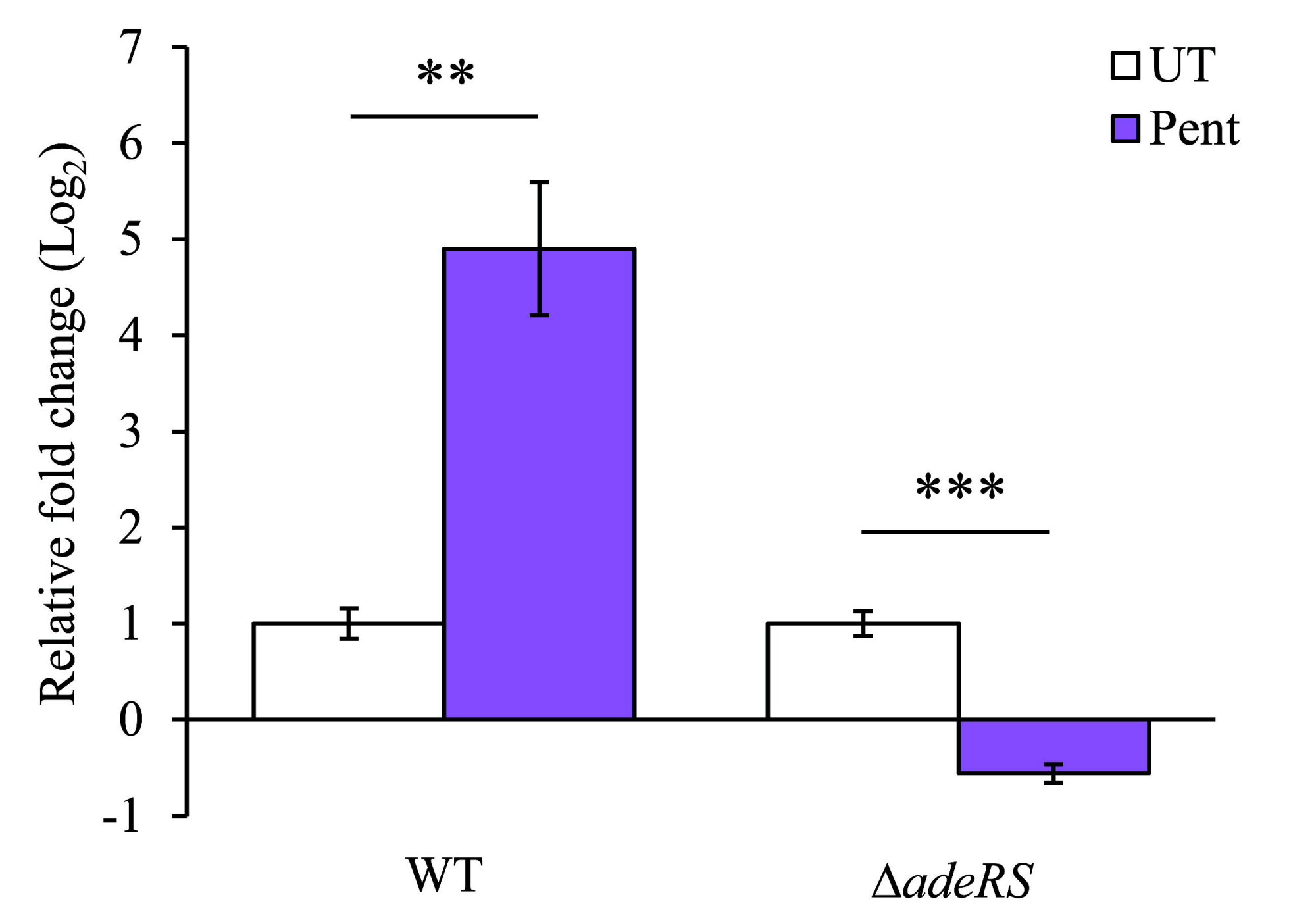
7
6
5
4
3
2
1
0
-1
Relative fold change (Log2)
**
***
UT
Pent
WT
ΔadeRS

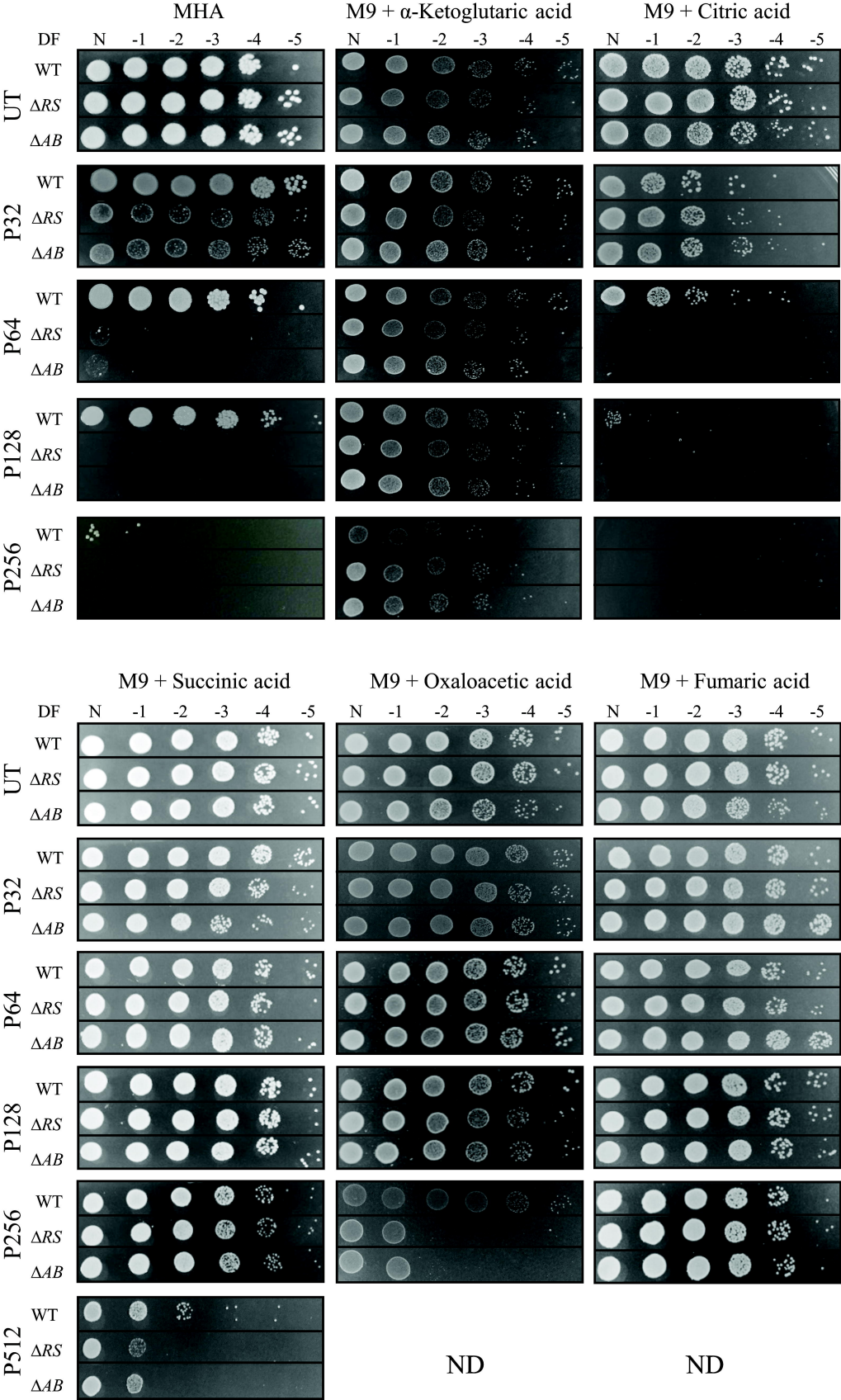
MHA
M9 + α-Ketoglutaric acid
M9 + Citric acid
M9 + Succinic acid
M9 + Oxaloacetic acid
M9 + Fumaric acid
DF
N -1 -2 -3 -4 -5
UT
P32
P64
P128
P256
P512
WT
ΔRS
ΔAB
ND
ND

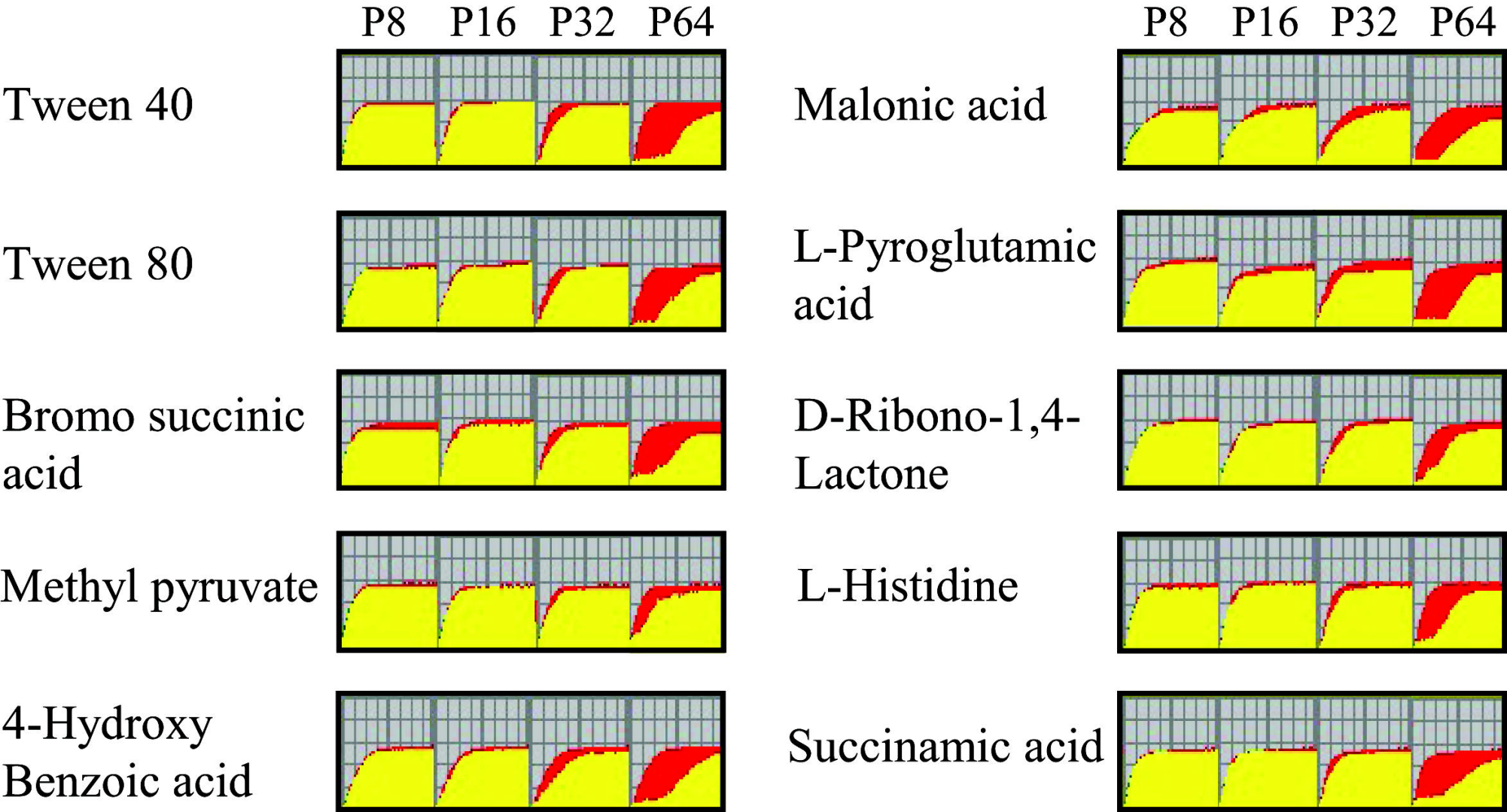
P8
P16
P32
P64
Tween 40
Tween 80
Bromo succinic acid
Methyl pyruvate
4-Hydroxy Benzoic acid
P8
P16
P32
P64
Malonic acid
L-Pyroglutamic acid
D-Ribono-1,4-Lactone
L-Histidine
Succinamic acid